

Standard molar enthalpies of formation of 3-methylglutaric and 3,3-dimethylglutaric anhydrides

M. A. García-Castro*, F. Díaz-Sánchez, J. A. Galicia-Aguilar and E. Vidal-Robles
*Facultad de Ingeniería Química de la Benemérita Universidad Autónoma de Puebla,
18 Sur y Av. San Claudio Ciudad Universitaria, 72570, Puebla, Pue, México.*
*e-mail: miguel.garciacastro@correo.buap.mx

Received 6 September 2022; accepted 12 March 2023

In this research, both the standard molar enthalpy of formation in the crystalline phase and in the gas phase of 3-methylglutaric anhydride was calculated from experimental data. The temperature and enthalpy of fusion, as well as the molar heat capacity in solid phase was calculated by differential scanning calorimetry; the molar enthalpy of sublimation at 298.15 K by the Knudsen effusion method, the molar enthalpy of vaporization at 298.15 K by thermogravimetric analysis, and the standard massic combustion energy by combustion adiabatic calorimetry. Since 3,3-dimethylglutaric anhydride presented crystal transitions (with endothermic points at 352.76 K, 356.98 K and 397.15 K), some of its thermochemical properties were estimated from the functional group-contribution methods proposed by Benson, Gani and Naef and from application of Machine Learning based models.

Keywords: 3-methylglutaric anhydride; 3,3-dimethylglutaric anhydride; enthalpy of formation; functional group-contribution methods.

DOI: <https://doi.org/10.31349/RevMexFis.69.051701>

1. Introduction

Cyclic acid anhydrides have been used as tools for bioconjugation [1], in the field of catalysts [1–6], in food chemistry [7], for cancer immunotherapy [8], in the synthesis of herbicides [9], for the preparation of membranes [10], in the green synthesis of macromolecules and nanoparticles [11, 12], in the polymer and copolymer area [13–15], among other applications. Moreover, some cyclic anhydrides present unusual physical behavior and polymorphic phase transitions in crystalline phase whose properties have been obtained by differential scanning calorimetry and powder X-ray diffraction [16–18]. Thermal and calorimetric analyses have been applied in investigations for material characterizations [19, 20] and on obtaining properties of polymorphic organic compounds based on previously established methodologies [21–23].

The standard molar enthalpies of formation are of the utmost importance since they generally are occupied to determine standard molar enthalpies of reaction and, thus, anticipate the exothermic or endothermic nature of a process [13]. Unfortunately, thermochemical properties of certain compounds cannot be obtained experimentally since they decompose during thermal analysis or, when appropriate, they show different transitions during their heating [24]. Therefore, it is necessary to fall back on the application of functional group contribution methods and machine-learning-based models, procedures useful in chemical engineering [25, 26]. Among cyclic anhydride derivatives whose standard molar enthalpies of formation had not been determined until reported in this research, are 3-methylglutaric and 3,3-dimethylglutaric anhydrides, Fig. 1.

To 3-methylglutaric anhydride (MGA) the melting point, enthalpy of fusion and molar heat capacity in crystal phase, were obtained by differential scanning calorimetry (DSC). The molar enthalpies of sublimation and vaporization at 298.15K were determined by Knudsen effusion method and by thermogravimetric analysis (TGA), respectively. The standard molar enthalpy of formation in gas phase at 298.15K was calculated from the standard molar enthalpy of sublimation and formation in the crystal phase at 298.15K. This value together with the one of glutaric anhydride (GA) [27], were occupied to validate the functional group contribution methods used to estimate some thermochemical properties of 3,3-dimethylglutaric anhydride (DMGA), which showed drawbacks during purification and, therefore, in all its experimental analysis. Finally, a statistical method applying a multiple linear regression model based on machine learning was applied to estimate the enthalpy of formation in gas phase to DMGA.

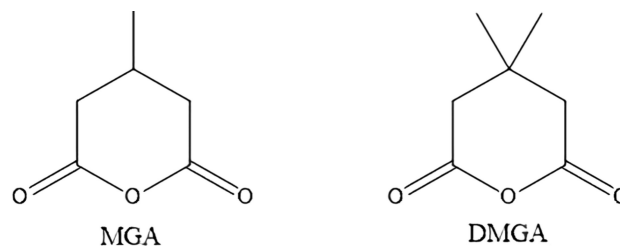


FIGURE 1. Representation of cyclic anhydrides, 3-methylglutaric (MGA) and 3,3-dimethylglutaric anhydride (DMGA).

2. Experimental

2.1. Materials and purity control

MGA [CAS: 4166-53-4] and DMGA [CAS: 4160-82-1] were acquired from Sigma-Aldrich, the mole-fraction purities reported by them were 0.98 and 0.99, respectively. The device occupied to calculate temperature and molar enthalpy of fusion was a Perkin Elmer DSC7 at a heating rate of 1.0 Kmin⁻¹ and a high purity nitrogen flow of 30.0 cm³min⁻¹ ($x = 0.99997$ and supplied by Infra Co.), this was calibrated for both temperature and heat flow using Indium metal [CAS: 7440-74-6] provided by NIST with mole fraction purity of 0.999999, fusion enthalpy of 28.6 Jg⁻¹ and melting point of 429.75 K [28–30].

MGA heat capacity was determined by DSC at a heating rate of 10.0 Kmin⁻¹ in a constant flow of nitrogen at 30.0 cm³min⁻¹ from 273.15 K to 304.15 K. The calibration was carried out with aluminum oxide [CAS: 1344-28-1, $x = 0.9995$] as a standard material provided by NIST, using the “two steps” method [31].

2.2. Combustion calorimetry

A Parr 1341 plain jacket adiabatic calorimeter was used for the combustion experiments, the methodology of this technique has been detailed in previous research [13]. The combustion energy of MGA was determined after calibration with benzoic acid as calorimetric standard of NIST (Standard Material Reference 39j), the certified massic energy of combustion of this standard of $-(26434.0 \pm 3.0)$ Jg⁻¹ (the uncertainty is the standard deviation of the mean) was corrected from the equation made available by Coops [32]. The energy equivalent of $\varepsilon(\text{calor}) = (9930.1 \pm 2.2)$ JK⁻¹ obtained from five calibration runs was made known in previous work [11], the uncertainty is twice the standard deviation of the average.

The combustion experiments of MGA were performed using a 0.022 L capacity bomb filled with high purity oxygen ($x = 0.99996$, supplied by Infra. Group) at a pressure of 3.04 MPa. In each test 0.1 cm³ of deionized water was occupied, approximately 1.1 g of MGA, 13.15 g of nichrome (with burning energy of $\Delta_c u^\circ(\text{nichrome}) = -(5857.6 \pm 1.0)$ Jg⁻¹ where the uncertainty is the standard deviation of the average). Besides, 4.184 J of ΔU_{ign} were provided by an ignition unit (Parr 2901). The energy of nitric acid formation during combustion was determined by titration, the value used of heat liberated in the formation of 0.1N HNO₃ under bomb conditions was $\Delta U_{\text{dec}}(\text{HNO}_3) = -59.7$ kJmol⁻¹ [33]. A 6775 Digital thermometer (from 10 to 40°C, inaccuracy: $\pm 0.001^\circ\text{C}$) was used to measure the temperature, and a digital multimeter HP 34420 A to register the resistance.

The physical properties of some materials were considered to correct ΔU^{exp} (Eq. (1)) to $\Delta_c U^\circ(298.15 \text{ K})$ (Eq. (2)). MGA ($M = 128.1338$ gmol⁻¹ [34], $\rho = 1.159$ gmL⁻¹ (value calculated using Advanced Chemistry Development (ACD/Labs) Software V11.02 (©1994-2022 ACD/Labs), $-(\delta u/\delta p)_T = 0.200$ Jg⁻¹ MPa⁻¹ [35], $C_p(\text{cr}, 298.15 \text{ K}) =$

1.405 ± 0.104 Jg⁻¹K⁻¹ (experimental average value from two experiments using DSC device. Its uncertainty corresponds to expanded uncertainty with a level of confidence of approximately 95%)), benzoic acid ($M = 122.1220$ gmol⁻¹ [34], $\rho = 1.320$ gmL⁻¹ [35], $-(\delta u/\delta p)_T = 0.115$ Jg⁻¹MPa⁻¹ [35], $C_p(\text{cr}, 298.15 \text{ K}) = 1.209$ Jg⁻¹K⁻¹ [35], stainless-steel ($\rho = 7.915$ gmL⁻¹ (Value provided by Parr for 45C10), $-(\delta u/\delta p)_T = 0.200$ Jg⁻¹MPa⁻¹ [35], $C_p(\text{cr}, 298.15 \text{ K}) = 0.500$ Jg⁻¹K⁻¹ (value provided by Parr for 45C10)), and nichrome ($M = 57.3670$ gmol⁻¹ [34], $\rho = 8.558$ gmL⁻¹ (value provided by Parr for 45C10), $-(\delta u/\delta p)_T = 0.200$ Jg⁻¹MPa⁻¹ [35], $C_p(\text{cr}, 298.15 \text{ K}) = 0.450$ Jg⁻¹K⁻¹ (value provided by Parr for 45C10)).

$$\Delta U^{\text{exp}} = -[\varepsilon(\text{calor})(-\Delta T_{ad}) + \Delta U_{\text{dec}}(\text{HNO}_3) + \Delta U_{\text{ign}} + m(-\Delta_c u^\circ)(\text{nichrome})], \quad (1)$$

$$\Delta_c U^\circ(298.15 \text{ K}) = -(m\Delta_c u^\circ)(298.15 \text{ K}) = \Delta U^{\text{exp}}, \quad (2)$$

$$\begin{aligned} -\varepsilon(\text{cont})(-\Delta T_{ad}) - \Delta U_{\text{corr}}\varepsilon(\text{cont})(-\Delta T_{ad}) \\ = \varepsilon_f(\text{cont})(298.15 \text{ K} - T_f + \Delta T_{\text{corr}}) \\ + \varepsilon_i(\text{cont})(T_i - 298.15 \text{ K}). \end{aligned} \quad (3)$$

where $\varepsilon(\text{cont})$ is bomb content energy (Eq. (3)), $\varepsilon_i(\text{cont})$ and $\varepsilon_f(\text{cont})$ are the energy equivalents of the bomb contents in the initial and final states, T_i and T_f are the initial and final temperatures of experiment and ΔU_{corr} is the correction to standard state.

2.3. Thermogravimetry using the Langmuir method

To estimate the enthalpy of vaporization, the procedure described by Price [36] applying the Langmuir equation was used:

$$(dm/dt)(1/A) = p \cdot \alpha(M/2\pi RT)^{1/2}, \quad (4)$$

where (dm/dt) is the rate of mass loss, A is the vaporization area, p is the vapor pressure, T is the absolute temperature, M is the molar mass, R is the gas constant, and α is the vaporization coefficient (equivalent to 1 when it comes to macromolecules or under vacuum conditions).

One way to determine the enthalpy of phase change from the vapor pressure is by combining the Langmuir and Clausius-Clapeyron equations, so that the Eq. (5) is obtained:

$$\ln(dm/dt)(1/A)(T/M)^{1/2} = C - (\Delta_l^g H_m)(1/T), \quad (5)$$

where C groups the involved constants and $\Delta_l^g H_m$ is the enthalpy of vaporization at average temperature T_m . For this investigation, as the loss of mass occurs after the melting temperature, the vaporization enthalpy was determined directly from the analysis of the MGA thermogram at T_m and later corrected to 298.15 K.

A TA instruments SDT 600 TGA/DSC was used for this procedure, its characteristics are reported in the literature [37]. The device calibration was performed for mass, temperature, and enthalpy of vaporization. Mass calibration was carried out with a standard provided and certified by the NIST as (315.162 ± 0.0048) mg. Temperature and heat flow calibration was carried out with high purity indium, this standard presents a NIST certified temperature of (429.7485 ± 0.00034) K and enthalpy of fusion of (28.51 ± 0.19) Jg⁻¹. During the calibrating was obtained a k (calibration constant) of 1.0000, determined from the fusion enthalpy. The nitrogen flow of 100 cm³ min⁻¹ and heating rate of 10 Kmin⁻¹ were obtained by different experimental tests with pyrene [CAS: 129-00-0, $x = 0.9996 \pm 0.0003$] and phenanthrene [CAS: 85-01-8, $x = 0.9997 \pm 0.0001$]. The vaporization enthalpy of (89.5 ± 1.4) kJmol⁻¹ to pyrene and (79.5 ± 1.4) kJmol⁻¹ to phenanthrene were compared with those reported in the literature, obtaining approximate values.

2.4. Knudsen effusion method

Another way to calculate the vapor pressure from the rate of mass loss was through the Knudsen effusion equation:

$$p = (\Delta m / \Delta t / w_0 A_0) (2\pi RT / M)^{1/2}, \quad (6)$$

where $\Delta m / \Delta t$ is the rate of mass loss, T is absolute temperature, w_0 is the Clausing probability factor, A_0 is the effusion area, R is the ideal gas constant, and M is the molar mass.

Equation (7) obtained by combining the previous expression with the Clausius-Clapeyron equation, allowed to determine the enthalpy of sublimation $\Delta_{cr}^g H_m$, the details of experimental method have been described in previous studies [36].

$$\ln(\Delta m / \Delta t) \cdot T^{1/2} = \ln(1/w_0 A_0) (2\pi R / M) - (\Delta_{cr}^g H_m / R) (1/T), \quad (7)$$

The rate of mass loss ($\Delta m / \Delta t$) at constant temperature was determined from 300.66 K to 306.54 K with steps of 2.0 K and using a vacuum pressure of 10⁻⁶ Torr, this value was utilized to calculate the enthalpy of sublimation. The experiments were carried using aluminum cells with a silver pierced disk whose measures were: Cell A (diameter: 1.345 mm, A_0 : 1.42 mm², thickness: 0.150 mm, w_0 factor: 0.9228), Cell B (diameter: 1.031 mm, A_0 : 0.835 mm², thickness: 0.135 mm, w_0 factor: 0.9106), Cell C (diameter: 0.842 mm, A_0 : 0.557 mm², thickness: 0.135 mm, w_0 factor: 0.8927) and Cell D (diameter: 0.489 mm, A_0 : 0.188 mm², thickness: 0.170 mm, w_0 factor: 0.7932). The temperature was recorded with a Hart Scientific thermistor model A1143-01 connected to an Agilent multimeter model 34420A. Two VARIAN vacuum pumps (model DS102 and V70D) were used to create a pumping system. The method validation was carried out by determining the sublimation enthalpy of two standards, ferrocene [CAS: 102-54-5, $x = 0.9997 \pm 0.0003$]

and anthracene [CAS: 120-12-7, $x = 0.9998 \pm 0.0003$], whose experimental values were (73.4 ± 2.2) kJmol⁻¹ and (104.2 ± 3.2) kJ mol⁻¹, respectively. The experimental values were approximate to those reported in the literature [39–49].

2.5. Estimation methods by contribution of functional groups

Since the enthalpy of formation in both gas and crystalline phases of the compound DMGA could not be determined experimentally due to the presence of three endothermic signals (at 352.76 K, 356.98 K and 397.15 K) before and after purification, three estimation methods proposed by Gani [50], Benson [51–53] and Naef [54, 55] were used to calculate the enthalpy of formation. The method validation was carried out from properties estimation of cyclic acid anhydrides derivatives, including GA and MGA. The procedure has already been described in detail by this research group [11].

Gani's method [50] separates the functional groups of each molecule into different orders (first, second and third order). This method requires using a H_{f0} value (42.2361 kJ mol⁻¹) for the estimated enthalpy of formation in gas phase. Benson's method [51–53] allows to estimate the enthalpy obtaining a theoretical value by locating the different atoms within a molecule (except for hydrogen) and by observing which atom is bonded to the one being studied, for the case of cyclic molecules, it is necessary to introduce a ring strain correction factor (rsc). In Naef's method [54, 55] the estimate enthalpy of formation in the crystalline phase is made from the enthalpy of combustion, and the estimated enthalpy of formation in the gas phase is calculated from sublimation enthalpy.

2.6. Theoretical results using statistical algorithms

One way to find theoretical values of enthalpy of formation in the gas phase, is applying statistical methods, these methods allow the interpretation of experimental results from another point of view, for this purpose machine learning algorithms were used [56].

2.6.1. Multiple linear regression

This regression model is characterized by the inclusion of multiple regressor variables, in other words, the dependent variable is not affected by only one independent variable. The expression representing this adjustment is presented below.

$$y = a_0 + a_1 X_1 + a_2 X_2 + \dots + a_n X_n \quad (8)$$

The model relates a dependent variable with n regressor variables (X_n) and finally a random variable (a_0) that collects all those factors that are not collectable and are associated to change [57].

2.6.2. Ridge regression

Ridge regression is a popular parameter estimation method used to address the collinearity problem frequently arising in multiple linear regression [58]. The expression representing this adjustment is presented below.

$$RSS_{Ridge} = \sum_{i=1}^n (y_i - f(x_i))^2 + \frac{1}{2} \lambda \sum_{j=1}^p \beta_j^2 \quad (9)$$

where λ is a parameter that controls the degree of penalty: the higher the penalty, the lower the coefficients, the more robust to collinearity. When λ is equal to zero, Ridge is equivalent to linear regression.

2.6.3. Lasso regression

LASSO (Least Absolute Shrinkage and Selection Operator) regression aims to identify the variables and corresponding regression coefficients that lead to a model that minimizes the prediction error. This is achieved by imposing a constraint on the model parameters, which ‘shrinks’ the regression coefficients towards zero, that is by forcing the sum of the absolute value of the regression coefficients to be less than a fixed value (λ) [59]. The expression representing this adjustment is presented below.

$$RSS_{Lasso} = \sum_{i=1}^n (y_i - f(x_i))^2 + \lambda \sum_{j=1}^p |\beta_j|, \quad (10)$$

where λ is a parameter that controls the degree of penalty: the higher the penalty, the lower the coefficients, the more robust to collinearity. When λ is equal to zero, Lasso is equivalent to linear regression.

3. Results and discussion

From three experiments of MGA the molar fraction, the temperature and molar fusion enthalpy, as well as heat capacity were determined by using DSC device. The molar fraction of MGA after recrystallization from ethyl ether had an average value of (0.9996 ± 0.0001) . The values obtained to temperature and molar fusion enthalpy were of (316.05 ± 0.01) K or (42.9 ± 0.01) °C and (15.75 ± 0.37) kJ mol⁻¹, respectively, and heat capacity as a function of the temperature in the range from 273.15 K to 304.15 K was of (180.0 ± 13.2) J mol⁻¹K⁻¹. The results showed an uncertainty of 0.95 and corresponds to the expanded uncertainty. To DMGA, even enough and various purification tests using different solvents in each one were done, three endothermic signals appeared at 352.76 K (79.61°C), 356.98 K (83.83°C) and 397.15 K (124.0°C), respectively, Fig. 2. Due to these crystal transitions possibly related to the different molecular shape as conformations, conformers or polymorphs neither the temperature nor the enthalpy of fusion could be determined from this technique.

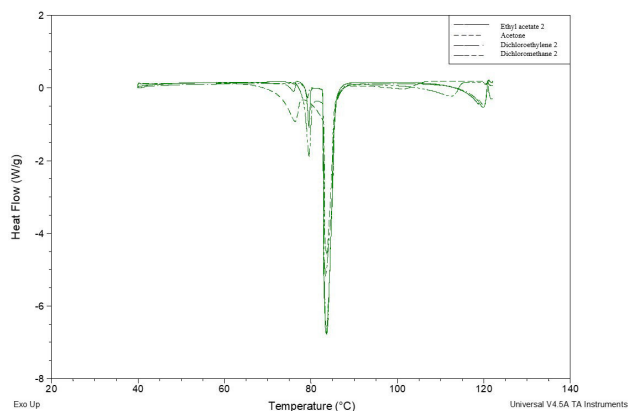
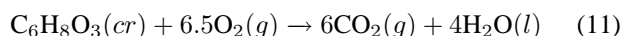


FIGURE 2. Endothermic signals to 3,3-dimethylglutaric anhydride.

Table I shows the data and average value of $\Delta_c U_m^\circ$ (MGA) at 298.15 K of five combustion experiments, the standard molar energy and enthalpy of combustion calculated from this was $\Delta_c U_m^\circ(298.15 \text{ K}) = -(2850.2 \pm 1.9)$ kJmol⁻¹ and $\Delta_c H_m^\circ(298.15 \text{ K}) = -(2851.4 \pm 1.9)$ kJmol⁻¹, respectively (where the uncertainty corresponds to the expanded uncertainty of five combustion experiments with confidence level of 95% and include the calibration contributions from benzoic acid and energy of combustion of nichrome thread). Finally, the enthalpy of formation in solid phase of MGA of $\Delta_f H_m^\circ(\text{cr}, 298.15 \text{ K}) = -(653.0 \pm 2.1)$ kJ mol⁻¹ was obtained taking into consideration the values of the enthalpies of formation in standard state for H₂O (l) of $-(285.83 \pm 0.04)$ kJ mol⁻¹ and for CO₂ (g) of $-(393.51 \pm 0.13)$ kJmol⁻¹ [58] (the uncertainty of $\Delta_f H_m^\circ(\text{cr})$ corresponds to the expanded uncertainty with confidence level of 95% and includes the uncertainties of standard enthalpy of formation of H₂O (l) and CO₂ (g)). The idealized reaction occupied is presented in Eq. (11).



The rate of mass loss (dm/dt) in the range of temperature from 339.15 K to 389.15 K was determined by using TGA, and from 300.66 to 306.54 K via Knudsen effusion. From these data, it was possible to obtain the vaporization enthalpy at average temperature of $T_m = 364.15$ K and the sublimation enthalpy at $T_m = 303.42$ K, respectively. These vaporization and sublimation enthalpies at T_m were corrected at 298.15 K, using equation series (12) and (13). These values are shown in the Table II (the uncertainties of enthalpies of sublimation and vaporization at T_m correspond to weighted average at 298.15 K to twice the combined standard).

$$\begin{aligned} \Delta_l^g H_m(298.15\text{K})/\text{kJ} \cdot \text{mol}^{-1} &= \Delta_l^g H_m(364.15\text{K}) \\ &+ \{10.58 + 0.26 \cdot [(0.85(C_{p,m}(\text{cr}, 298.15\text{K}) + 9.83) \\ &/0.74/\text{J} \cdot \text{mol}^{-1} \cdot \text{K}^{-1})]\} \\ &/1000 \cdot (364.15 \text{ K} - 298.15 \text{ K}) \end{aligned} \quad (12)$$

TABLE I. Combustion experiments at 298.15 K and $p^\circ = 0.1 \text{ MPa}^a$.

	Exp. 1	Exp. 2	Exp. 3	Exp.4	Exp.5
m (MGA)/g	1.10927	1.16778	1.15478	1.17958	1.18016
m (stainless-steel)/g	13.35335	13.35335	13.3598	13.35721	13.35438
m (nichrome)/g	0.01303	0.0129	0.01251	0.01343	0.01283
T_i /K	292.5789	292.5857	292.6173	292.5802	292.5706
T_f /K	295.0831	295.2194	295.2194	295.2432	295.2344
ΔT_{corr} /K	0.0126	0.0132	0.0130	0.0134	0.0134
ΔT_{ad} /K	2.4916	2.6205	2.5891	2.6496	2.6504
$\varepsilon(\text{calor})(-\Delta T_{ad})/\text{kJ}$	-24.7418	-26.0218	-25.7100	-26.3108	-26.3187
$\varepsilon_i(\text{cont})/\text{kJ K}^{-1}$	0.0185	0.0186	0.0186	0.0186	0.0186
$\varepsilon_f(\text{cont})/\text{kJ K}^{-1}$	0.0200	0.0201	0.0201	0.0202	0.0202
$\varepsilon(\text{cont})(-\Delta T_{ad})/\text{kJ}$	-0.0415	-0.0443	-0.0437	-0.0446	-0.0446
$\Delta U_{\text{ign}}/\text{kJ}$	0.0042	0.0042	0.0042	0.0042	0.0042
$\Delta U^{\text{exp}}/\text{kJ}$	24.6607	25.9411	25.6316	26.2261	26.2382
$\Delta U_{\text{dec}}(\text{HNO}_3)/\text{kJ}$	0.0006	0.0009	0.0009	0.0018	0.0012
$\Delta U_{\text{corr}}/\text{kJ}$	0.0169	0.018	0.0178	0.0182	0.0182
$(-m\Delta_c u^\circ)(\text{nichrome})/\text{kJ}$	0.0763	0.0756	0.0733	0.0787	0.0752
$(-m\Delta_c u^\circ)(\text{MGA})/\text{kJ}$	24.6853	25.9674	25.6575	26.2525	26.2645
$\Delta_c u^\circ(\text{MGA})/\text{kJ g}^{-1}$	-22.2536	-22.2366	-22.2185	-22.2558	-22.2550

Average value $\Delta_c u^\circ(\text{MGA})/\text{kJ g}^{-1} - 22.2439 \pm 0.0163$

^aData from five representative experiments where the specific energies of combustion at 298.15 K and 0.1 MPa are displayed, m represents the mass of MGA, stainless steel, and nichrome, the masses were corrected for buoyancy using densities of each one; T_i and T_f are the initial and final temperatures of the experiment, ΔT_{corr} is a correction term, ΔT_{ad} is the corrected temperature rise calculated by $\Delta T_{ad} = T_f - T_i - \Delta T_{\text{corr}}$; $\varepsilon(\text{calor})$ represents the energy equivalent of the entire system, $\varepsilon_i(\text{cont})$ and $\varepsilon_f(\text{cont})$ are the energy equivalents of the bomb contents in the initial and final states, respectively; $\varepsilon(\text{cont})$ is bomb content energy calculated by $\varepsilon(\text{cont})(-\Delta T_c) = \varepsilon_i(\text{cont})(T_i - 298.15 \text{ K}) + \varepsilon_f(\text{cont})(298.15 \text{ K} - T_f + \Delta T_{\text{corr}})$, ΔU_{ign} is the ignition energy, $\Delta U_{\text{dec}}(\text{HNO}_3)$ is the experimental energy of formation of nitric acid, ΔU^{exp} the energy of the experimental bomb process, which was calculated by $\Delta U^{\text{exp}} = -[\varepsilon(\text{calor})(-\Delta T_c) + \Delta U_{\text{dec}}(\text{HNO}_3) + \Delta U_{\text{ign}} + (-m\Delta_c u^\circ)(\text{nichrome})]$, ΔU_{corr} is the correction to standard state and $\Delta_c u^\circ(\text{MGA})$ is the compound mass energy of combustion. Its uncertainty corresponds to expanded uncertainty with a confidence level of 0.95 approximately.

TABLE II. Sublimation and vaporization enthalpies for MGA.

$\Delta_\alpha^\beta H_m(T_m/\text{K})$ kJ mol ⁻¹	Interval of T/K	T_m/K	$\Delta_\alpha^\beta H_m(298.15 \text{ K})$ kJ mol ⁻¹	Method	Process
61.1 ± 0.3	339.15-389.15	364.15	65.6 ± 0.6	TGA	Vaporization
81.8 ± 1.7	300.66-306.54	303.42	81.9 ± 3.4	Knudsen effusion	Sublimation

$$\begin{aligned} \Delta_{cr}^g H_m(298.15 \text{ K})/\text{kJ} \cdot \text{mol}^{-1} &= \Delta_{cr}^g H_m(303.42 \text{ K}) \\ &+ \{0.75 + 0.15 \cdot [C_{p,mcr}, 298.15 \text{ K}]/J \cdot \text{mol}^{-1} \cdot \text{K}^{-1}\} \\ &/1000 \cdot (303.42 \text{ K} - 298.15 \text{ K}) \end{aligned} \quad (13)$$

Table III compare the enthalpy of sublimation at 298.15 K obtained by Knudsen effusion with the adding the vaporization enthalpy and the fusion enthalpy at 298.15 K, having a difference of 1.3 kJmol^{-1} (all the uncertainties correspond to twice the combined standard). This procedure was validated

with pyrene (with a difference of 0.3 kJmol^{-1}) and phenanthrene

TABLE III. Comparison of sublimation enthalpies at $T = 298.15 \text{ K}$.

$\Delta_{cr}^l H_m(T)$ kJ mol ⁻¹	$\Delta_f^g H_m(T)$ kJ mol ⁻¹	$\Delta_{cr}^g H_m(T)$ kJ mol ⁻¹	$\Delta_{cr}^l H_m(T)$ + $\Delta_f^g H_m(T)$ kJ mol ⁻¹
	TGA	Knudsen effusion	
15.0 ± 0.4	65.6 ± 0.6	81.9 ± 3.4	80.6 ± 0.7

TABLE IV. Functional groups occupied by method.

Benson estimation		Gani estimation		Naef estimation		
<i>MGA</i>						
Groups	Freq.	Groups	Freq.	Atom type	Neighbours	Freq.
C-(H) ₃ (C)	1	CH ₃	1	C sp ³	H ₃ C	1
CH ₃ corr (ter)	1	CH ₂ (cyclic)	2	C sp ³	HC ₃	1
C-(C) ₃ (H)	1	CH(cyclic)	1	C sp ³	H ₂ C ₂	2
C-(CO)(C)(H) ₂	2	CO(cyclic)	2	C sp ²	CO=O	2
CO-(C)(O)	2	O(cyclic)	1	O	C ₂ (2pi)	1
O-(CO) ₂	1	CH(cyclic)-CH ₃	1			
rsc GA	1					
<i>DMGA</i>						
Groups	Freq.	Groups	Freq.	Atom type	Neighbours	Freq.
C-(H) ₃ (C)	2	CH ₃	2	C sp ³	H ₃ C	2
CH ₃ corr (qua)	2	CH ₂ (cyclic)	2	C sp ³	C ₄	1
C-(C) ₄	1	C(cyclic)	1	C sp ³	H ₂ C ₂	2
C-(CO)(C)(H) ₂	2	CO(cyclic)	2	C sp ²	CO=O	2
CO-(C)(O)	2	O(cyclic)	1	O	C ₂ (2pi)	1
O-(CO) ₂	1	C(cyclic)-CH ₃	1			
rsc GA	1					

TABLE V. Comparison of estimated and experimental values of $\Delta_f^g H_m(298.15 \text{ K})$ and $\Delta_{cr}^g H_m(298.15 \text{ K})$ in kJmol^{-1} by Naef's method.

Compound	Experimental		Estimations			
	Vaporization	Sublimation	Vaporization	Δ	Sublimation	Δ
Glutaric acid	101.6 ± 0.8 ^a	119.2 ± 1.4 ^a	90.4	11.2	105.1	14.1
Maleic anhydride	43.8 ± 3.0 ^b	68.8 ± 0.8 ^c	50.5	-6.7	54.3	14.5
GA	52.6 ± 3.0 ^b	86.1 ± 1.6 ^d	54.4	-1.8	97.0	-10.9
3,3-Tetramethyleneglutaric anhydride	81.1 ^e	96.4 ± 1.1 ^e	70.3	10.8	81.1	15.3
Succinic anhydride	49.9 ± 3.0 ^b	80.7 ± 1.6 ^d	46.6	3.3	57.8	22.9
Methylsuccinic anhydride	47.6 ± 3.0 ^b	50.0 ^f	51.7	-4.1	59.2	-9.2
2,2-Dimethylsuccinic anhydride	45.7 ± 3.0 ^b	69.7 ^g	50.0	-4.3	58.7	11.0
MGA	65.6 ± 0.6 ^h	81.9 ± 3.4 ^h	56.4	9.2	98.3	-16.4
DMGA			57.8		97.8	

^aTaken on Ref. [61]. ^bTaken on Ref. [62]. ^cTaken on Ref. [63]. ^dTaken on Ref. [64]. ^eTaken on Ref. [27]. ^fCalculated from Refs. [62] and [65]. ^gCalculated from Refs. [53] and [66]. ^hExperimental value of this work.

$$\begin{aligned} \Delta_{cr}^l H_m(298.15 \text{ K}) &= \Delta_{cr}^l H_m(T_{fus}/K) + \{0.75 \\ &+ 0.15[C_{p,m}(cr, 298.15 \text{ K})/J \cdot \text{mol}^{-1} \cdot \text{K}^{-1}]\} \\ &/1000 \cdot (T_{fus}/K - 298.15K) - \{10.58 \\ &+ 0.26[C_{p,m}(l, 298.15K)]/J \cdot \text{mol}^{-1} \cdot \text{K}^{-1}\} \\ &\cdot (T_{fus}/K - 298.15 \text{ K}). \end{aligned} \quad (14)$$

To determine the enthalpy of formation in gas phase at 298.15 K of $-(571.1 \pm 4.0) \text{ kJ mol}^{-1}$ the Eq. (15) was ap-

plied, the value occupied of sublimation enthalpy was via Knudsen effusion where solid-gas equilibrium can be guaranteed. The uncertainties correspond to the expanded uncertainty with a level of confidence of approximately 0.95.

$$\Delta_f H_m^o(g, T) = \Delta_f H_m^o(cr, T) + \Delta_{cr}^g H_m(T), \quad (15)$$

where T represents the temperature at 298.15 K.

Table IV shows the functional groups and the frequency of appearing for MGA and DMGA, these data were applied to the three estimating methods.

TABLE VI. Comparison of estimated and experimental values of $-\Delta_c H_m^\circ$ in kJmol^{-1} by Naef's method.

Compound	Experimental	Estimations	Δ
Glutaric acid	2152.0 ± 0.5^a	2169.8	17.8
Maleic anhydride	1390.0 ± 1.4^b	1372.1	-17.9
GA	2206.5 ± 0.6^c	2196.3	-10.2
3,3-Tetramethyleneglutaric anhydride	4588.7 ± 2.1^d	4557.5	-30.6
Succinic anhydride	1537.1 ± 0.4^c	1543.8	6.7
Methylsuccinic anhydride	2208.0 ^e	2194.8	-9.2
2,2-Dimethylsuccinic anhydride	2855.0 ^e	2842.8	-12.2
MGA	2851.4 ± 1.9^f	2847.3	-4.1
DMGA		3495.3	

^aTaken on Ref. [61]. ^bTaken on Ref. [63]. ^cTaken on Ref. [64]. ^dTaken on Ref. [27]. ^eTaken on Ref. [66]. ^fExperimental value of this work.

TABLE VII. Comparison of estimated and experimental values of $-\Delta_f H_m$ (cr, 298.15 K) in kJ mol^{-1} by Benson and Naef methods.

Compound	Experimental	Benson	Δ	Naef	Δ
Glutaric acid	959.9 ^a	962.3	2.4	941.1	-18.5
Maleic anhydride	469.9 ± 1.5^b	469.9	0.0	487.8	17.9
GA	618.5 ^a	618.4	-0.1	628.8	10.3
3,3-Tetramethyleneglutaric anhydride	667.9 ± 2.4^c	678.6	10.7	699.1	31.2
Succinic anhydride	608.6 ± 0.7^d	601.6	-7	601.9	-6.7
Methylsuccinic anhydride	620.0 ± 1.2^e	622.8	2.8	630.3	10.3
2,2-Dimethylsuccinic anhydride	651.4 ^f	655.6	4.2	661.6	10.2
MGA	653.0 ± 2.1^g	650.4	-2.6	657.1	4.1
DMGA		688.7		688.5	

^aTaken on Ref. [68]. ^bTaken on Ref. [63]. ^cTaken on Ref. [27]. ^dTaken on Ref. [64]. ^eTaken on Ref. [65]. ^fTaken on Ref. [66]. ^gExperimental value of this work.

From Tables V to VIII the estimate values obtained by the functional group-contribution methods proposed by Benson, Gani and Naef, are shown. Tables V to VI present the values of vaporization, sublimation and combustion enthalpy obtained by Naef's method. To apply it in the estimated enthalpy of vaporization, a correction to O-C₂(2pi) group was made, whose value reported by Naef is -7.15 kJmol^{-1} [54]. However, if this quantity is used during the estimation of cyclic acid anhydrides, it generates a high absolute error. For this reason, the GAV for the O-C₂(2pi) group was recalculated from the subtraction between the experimental vaporization enthalpy and the theoretical vaporization enthalpy of each anhydride (without considering the recalculated group). Finally, the recalculated average value of 6.0 kJmol^{-1} was applied to estimate the vaporization enthalpy of all cyclic anhydrides. It was observed that the vaporization, sublimation, and combustion estimated enthalpies had an average error of 6.4 kJmol^{-1} , 14.3 kJmol^{-1} and 13.6 kJmol^{-1} , respectively. Considering the above values to DMGA a vaporization enthalpy of $(57.8 \pm 6.4) \text{ kJmol}^{-1}$, a sublimation enthalpy of $(97.8 \pm 14.3) \text{ kJmol}^{-1}$ and a combustion enthalpy of $-(3495.3 \pm 13.6) \text{ kJmol}^{-1}$, were estimated.

For the estimation of the enthalpies of formation in both gas and crystalline phases by the Benson's method [51–53], the rsc of maleic anhydride had to be calculated because it is not reported, the value obtained was 16.7 kJmol^{-1} for the gas phase and 19.7 kJmol^{-1} for the crystalline phase. A new GAV value was obtained [53] for the rsc cyclopentane because the reference [51] does not consider whether cyclopentane has radicals or not, likewise the reference [52] does not contain a value of rsc cyclopentane for the crystalline phase. The values used were 19.55 kJmol^{-1} for the gas phase and 34.0 kJmol^{-1} for the crystalline phase. Subsequently these values were used for the estimation of the compound 3,3-Tetramethyleneglutaric anhydride.

Table VII shows the results of enthalpy of formation in crystalline phase to DMGA calculated by Benson and Naef methods. Benson's method obtained a value of $-(688.7 \pm 3.7) \text{ kJmol}^{-1}$ while Naef method a value of $-(688.5 \pm 13.6) \text{ kJmol}^{-1}$.

Finally, in Table VIII are exposed the estimated enthalpies of formation in gas phase to DMGA by Benson, Gani, and Naef methods, obtaining values of $-(602.3 \pm 4.2) \text{ kJmol}^{-1}$, $-(579.1 \pm 8.0) \text{ kJmol}^{-1}$, and $-(590.7 \pm 17.2) \text{ kJmol}^{-1}$, respectively.

TABLE VIII. Comparison of estimated and experimental values of $-\Delta_f H_m$ (g, 298.15 K) in kJ mol^{-1} by Benson, Gani, and Naef methods.

Compound	Experimental	Benson	Δ	Gani	Δ	Naef	Δ
Glutaric acid	840.2 ± 4.6^a	842.5	2.3	843.5	3.3	835.9	-4.3
Maleic anhydride	401.0 ± 1.7^b	401.0	0.0	416.2	15.2	433.5	32.5
GA	532.4 ± 1.8^c	532.1	-0.3	541.9	9.5	531.8	-0.6
3,3-Tetramethyleneglutaric anhydride	571.5 ± 2.6^a	573.2	1.7	563.2	-8.3	618.0	46.5
Succinic anhydride	527.9^d	528.0	0.1	542.2	14.3	552.3	19.6
Methylsuccinic anhydride	570.0^e	557.4	-12.6	576.2	6.2	571.1	1.0
2,2-Dimethylsuccinic anhydride	581.7^f	590.1	8.4	579.5	-2.2	602.9	21.2
MGA	571.1 ± 4.0^g	562.5	-8.6	575.9	4.8	558.8	-12.3
DMGA		602.3		579.1		590.7	

^aTaken on Ref. [27]. ^bTaken on Ref. [63]. ^cTaken on Ref. [64]. ^dTaken on Ref. [69]. ^eCalculated from Refs. [62] and [65]. ^fTaken on Ref. [53]. ^gExperimental value of this work.

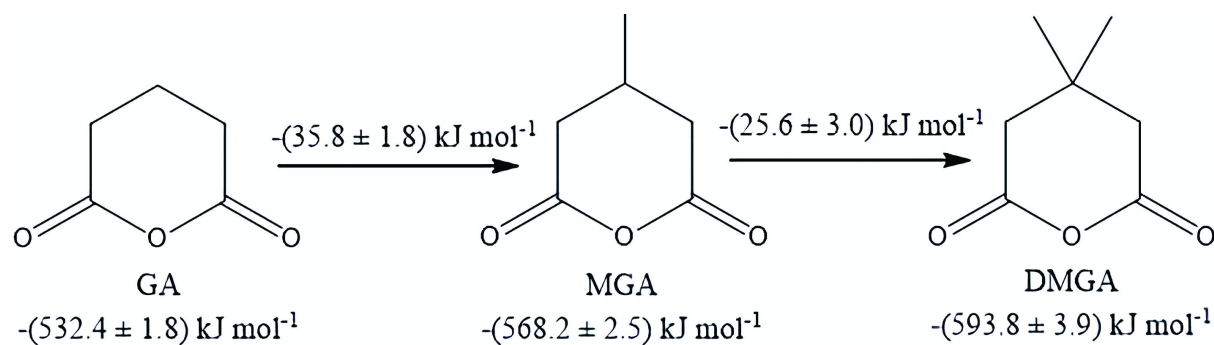


FIGURE 3. Values estimated from enthalpic contribution of methyl group.

Another way to estimate the enthalpy of formation in gas phase of DMGA was using the enthalpic contribution of the methyl group of $-35.8 \text{ kJ mol}^{-1}$ obtained from the difference between 4-methylpiperidine [70] and piperidine [71], and of $-25.6 \text{ kJ mol}^{-1}$ obtained from the difference between 2,2,6,6-tetramethylpiperidine [72] and 2,6-dimethylpiperidine [70]. The first value was applied on GA to calculate the estimated enthalpy of formation in gas phase at 298.15 K of MGA resulting in $\Delta_f H_m^\circ(\text{g}, 298.15 \text{ K}) = -(568.2 \pm 2.5) \text{ kJ mol}^{-1}$. It can be observed that there is a difference between the estimated and experimental value, of 2.9 kJ mol^{-1} . The second value was applied on MGA to estimate the enthalpy of formation in gas phase at 298.15 K of DMGA giving $\Delta_f H_m^\circ(\text{g}, 298.15 \text{ K}) = -(593.8 \pm 3.9) \text{ kJ mol}^{-1}$, it was observed a difference of 8.5 kJ mol^{-1} with regard to Benson method, of 14.7 kJ mol^{-1} related to Gani method, and of 3.1 kJ mol^{-1} compared to Naef method. The results are shown in Fig. 3.

To apply an algorithm based on machine learning, it was first necessary to create a database representative of the type of molecules studied in this work. The database created contains a total of 70 organic compounds divided between carboxylic acids and acid anhydrides, since an anhydride is a derivative of an acid, it can be considered that their molecular interactions are similar, each existing organic compound

within the database contains its respective enthalpy of formation in the gas phase.

A multiple Linear Regression, Ridge Regression and Lasso Regression models were applied in order to predict the enthalpy of formation in the gas phase based on the number of carbon, hydrogen and oxygen atoms, the originally created set was divided into two (training and test) with a value of 0.7 and 0.3 respectively and a seed was used to ensure that the results can be repeatable, likewise the evaluation metrics used to determine the effectiveness of the model were the coefficient of determination (R^2) whose methodology has already been explained previously [73], the root mean square error (RMSE) [74] and the mean absolute error (MAE) [75], likewise a cross validation (K-fold) [76] was applied to the training set in order to know its accuracy. The results, as well as the adjustment equation are presented in Table IX.

In the case of the hyperparameter Alpha present in both the Ridge Regression and the Lasso Regression during Python programming, a for loop was performed in order to evaluate the optimal value for this parameter, it was found that for both regressions the optimal value for alpha is in the interval of (0,2] because after 2 the value of the coefficient of determination begins to decay and 0 cannot be taken because it would become a multiple linear regression, for this work the value used in both cases was Alpha = 2.

TABLE IX. Results of Machine Learning.

Multiple Linear Regression										
	Training set	Test set		Training set	Test set		Training set	Test set		
R^2	0.9882	0.9836	MAE	13.2375	16.2029	RMSE	19.4279	21.6080	Cross val (std) ^b	0.9614
$y = -25.9068 - 32.9022x_1 + 28.2672x_2 + 193.1793x_3^a$										
Ridge Regression										
	Training set	Test set		Training set	Test set		Training set	Test set		
R^2	0.9846	0.9829	MAE	14.4831	15.4201	RMSE	22.1680	22.0452	Cross val (std) ^b	0.9619
$y = 22.0314 - 33.7033x_1 + 28.0985x_2 + 177.3040x_3^a$										
Lasso Regression										
	Training set	Test set		Training set	Test set		Training set	Test set		
R^2	0.9879	0.9833	MAE	12.9703	16.1354	RMSE	19.6778	21.7944	Cross val (std) ^b	0.9528
$y = -15.9902 - 32.4211x_1 + 27.9305x_2 + 189.1128x_3^a$										

^a x_1 represents the carbon atoms, x_2 the hydrogen atoms and x_3 the oxygen atoms present in the molecules coming from anhydrides, the results are in $\text{kJ}\cdot\text{mol}^{-1}$. ^bRepresents the mean of standard deviation with $cv = 10$.

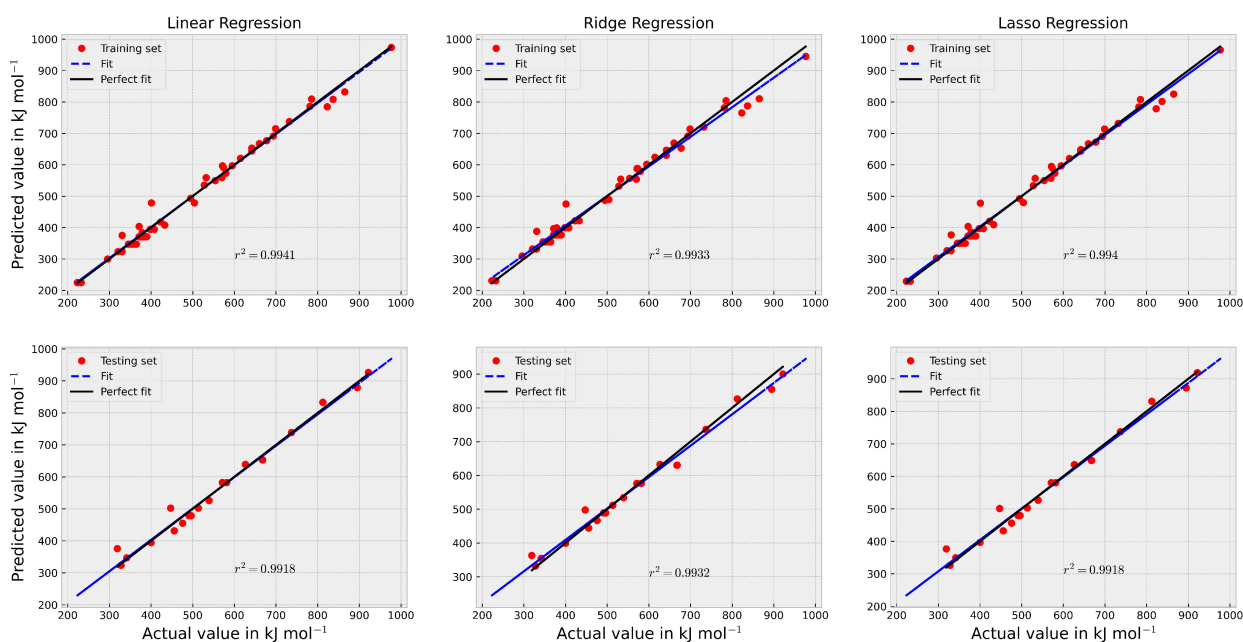


FIGURE 4. Comparison between true and predicted enthalpy of formation values.

Figure 4 shows the fits obtained using the different types of regression for both the training and test sets, as it can be seen the multiple linear regression and the lasso regression were the ones that had the best fit to the data set, the r^2 value refers to the coefficient of determination between the true data set and the predicted data set.

Based on the metrics shown in Table IX, the types of regression that present a better adjustment in general are Lasso Regression and Multiple Linear Regression, therefore, both adjustment equations will be used to predict the enthalpy of formation of DMGA. Since the equation presented in Table IX do not distinguish between isomerism, it is necessary

to introduce a correction factor, this factor was taken from the literature of the Benson type estimation method [53], the value considered was the quaternary $-\text{CH}_3$ correction in order to ensure that both methyl groups are attached to the same carbon atom. Using the equations presented in Table IX, the value of the enthalpy of formation in the gas phase of MGA gives a result of $-\Delta_f H^\circ(\text{MGA}, g) = 580.3 \text{ kJmol}^{-1}$ using the Lasso Regression, $-\Delta_f H^\circ(\text{MGA}, g) = 576.5 \text{ kJmol}^{-1}$ using the Ridge Regression and $-\Delta_f H^\circ(\text{MGA}, g) = 582.4 \text{ kJmol}^{-1}$ using the Multiple Linear Regression, comparing the values with the experimental value, shows a difference of 9.2 kJmol^{-1} , 5.4 kJmol^{-1} and 11.3 kJmol^{-1} using the

Lasso Regression, Ridge Regression and Multiple Linear Regression respectively, and DMGA gives as a result of $-\Delta_f H^\circ(\text{DMGA, g}) = 603.7 \text{ kJmol}^{-1}$ using the Lasso Regression, $-\Delta_f H^\circ(\text{DMGA, g}) = 599.0 \text{ kJmol}^{-1}$ using the Ridge Regression and $-\Delta_f H^\circ(\text{DMGA, g}) = 606.0 \text{ kJmol}^{-1}$ using the Multiple Linear Regression, the value of the correction factor is -4.56 kJmol^{-1} , this factor was applied twice due to the two methyl groups attached to the quaternary carbon, the final values result in $-\Delta_f H^\circ(\text{DMGA, g}) = 594.6 \text{ kJmol}^{-1}$, $-\Delta_f H^\circ(\text{DMGA, g}) = 589.9 \text{ kJmol}^{-1}$ and $-\Delta_f H^\circ(\text{DMGA, g}) = 596.9 \text{ kJmol}^{-1}$ with the Lasso Regression, Ridge Regression and the Multiple Linear Regression, respectively. Comparing the values with the one obtained in Fig. 3, shows a difference of 0.8 kJmol^{-1} , -3.9 kJmol^{-1} and 3.1 kJmol^{-1} using the Lasso Regression, Ridge Regression and Multiple Linear Regression respectively.

4. Conclusions

Some thermochemical properties of MGA were determined by applying differential scanning calorimetry, thermogravimetric analysis, and Knudsen's effusion method. Since DMGA could not be studied experimentally due to the ex-

istence of crystal transitions possibly related to the different molecular shape as conformations, conformers or polymorphs, the Benson, Gani, and Naef functional group-contribution methods were applied to calculate the enthalpies of phase change and formation in both the gas phase and the crystalline phase. Likewise, the standard molar enthalpy of formation was estimated in gas phase of DMGA from two ways 1) from enthalpic contribution of methyl group on GA and on MGA, and 2) from different linear regression algorithms applying Machine Learning. As it can be seen, the estimated enthalpy of formation in gas phase obtained by all methods, the differences between the values gathered fall within uncertainty. With regards to the estimated enthalpy of formation in crystalline phase, the values were very close by both the Benson and Naef method.

Acknowledgments

We are grateful for the facilities provided by VIEP project number 100420555-VIEP2022 "Mecanosíntesis y estudio termoquímico de la o-diimida diácida derivada del anhídrido ftálico".

1. V. S. Maria and B. Line, Cyclic anhydrides as powerful tools for bioconjugation and smart delivery, *Bioconjugate Chem.* **32** (2021) 482, <https://dx.doi.org/10.1021/acs.bioconjchem.1c00023>
2. J. C. Bardhan, R. N. Adhya and K. C. Bhattacharyya, Synthesis of polycyclic compounds. Part IV. Substituted 3-alkylphenanthrenes, *J. Chem. Soc.* (1956) 1346, <https://doi.org/10.1039/JR9560001346>
3. Y. Yamamoto, K. Yamamoto, T. Nishioka and J. Oda, Asymmetric synthesis of optically active lactones from cyclic acid anhydrides using lipase in organic solvents, *Agr. Biol. Chem.* **52** (2014) 3087, <https://doi.org/10.1080/00021369.1988.10869185>
4. R. C. Dale, Indoline compounds as granzyme b inhibitors. Patent No. US 10,329,324 B2; *PCT Int. Appl.* (2019)
5. T.Y. Wu, Y. R. Lai and S. W. Tsai, CALB-Catalyzed two-step alcoholic desymmetrization of 3-methylglutaric diazolides in MTBE, *Appl. Biochem. Biotech.* **185** (2018) 578, <https://doi.org/10.1007/s12010-017-2675-1>
6. J. H. Shim, S. J. Park, B. K. Ahn, J. Y. Lee, H. S. Kim and D. C. Ha, Enantioselective thiolysis and aminolysis of cyclic anhydrides using a chiral diamine-derived thiourea catalyst, *ACS Omega* **50** (2021) 34501, <https://doi.org/10.1021/acsomega.1c04741>
7. S. K. Gandhi, J. R. Schultz, F. W. Boughey and R. H. Forsythe, Chemical modification of egg white with 3,3-dimethylglutaric anhydride, *J. Food Sci.* **33** (1968) 163.
8. E. Yuba *et al.*, Dextran derivative-based pH-sensitive liposomes for cancer immunotherapy, *Biomaterials* **35** (2014) 3091, <http://dx.doi.org/10.1016/j.biomaterials.2013.12.024>
9. K. L. Kobrakov, V. K. Korolev, L. I. Rybina and V. I. Kelarev, Halogen-containing pyridines. 7. Synthesis and some conversions of (3,5-dichloro-2-pyridyl)hydrazine, *Chem. Heterocycl. Com+* **36** (2000) 931, DOI: 10.1007/bf02256977
10. T. Trang, N. Nhung and T. Kobayashi, Fabrication and characterization of pulp/chitosan composite membranes crosslinked with 3-methylglutaric anhydride for pervaporation of ethanol/water mixture, *Engineering-London* **3** (2011) 110, DOI: 10.4236/eng.2011.32014
11. K. Salas-López *et al.*, Standard enthalpies of formation of N,N'-(1,3-phenylene)bis(phthalimide) and N,N'-(1,3-phenylene)bis(phthalimide-5-carboxylic acid), *Thermochim. Acta.* **697** (2021) 178861, <https://doi.org/10.1016/j.tca.2021.178861>
12. M. Caldera, M. A. García-Castro, J. García and A. M. Herrera, Comparison of polyampholyte derivative of chitosan with bisphthalimides of low molecular weight in the green synthesis of Au nanoparticles, *Gold Bull.* **55** (2022) 41, <https://doi.org/10.1007/s13404-022-00310-2>
13. M. López-Badillo *et al.*, Experimental standard enthalpies of formation 4,4-methylenedi(phenylene isocyanate) and polyamide-imides, *Russ. J. Phys. Chem. B.* **15** (2021) S201, <https://doi.org/10.1134/S19907931211100067>
14. M. López-Badillo *et al.*, Obtaining kinetic parameters of polyamide imide reaction. *Rev. Mex. Ing. Química*, **19** (2019) 783, <https://doi.org/10.24275/rmiq/Cat606>

15. Z. Xun, Z. Chengjian and Z. Xinghong, A facile and unprecedented route to a library of thermostable formaldehyde-derived polyesters: highly active and selective copolymerization of cyclic acetals and anhydrides, *Angew. Chem-Ger Edit.* **61** (2022), <https://doi.org/10.1002/anie.202117316>
16. S. R. Jezowski, S. Monaco, H. P. Yennawar, N. M. Wonderling, R. T. Mathersd and B. Schatschneider, Unusual physical behaviour and polymorphic phase transitions in crystalline bicyclic anhydrides, *Cryst. Eng. Comm.* **19** (2017) 276, <https://doi.org/10.1039/C6CE02036D>
17. D. Zhao, F. F. Li and A. Y. Zhang, Naphthalene-1,8-dicarboxylic anhydride: a monoclinic polymorph, *Acta Cryst.* **66** (2010) o2622, <https://doi.org/10.1107/S1600536810037608>
18. G. Díaz, B. Ramírez V, W. Velásquez and P. Rodríguez, A new polymorph of 9,10-dihydroanthracene-9,10- α,β -succinic acid anhydride, *Acta Cryst.* **58** (2002), o501, <https://doi.org/10.1107/S1600536802005767>
19. M. Kuhnert-Brandstatter and H. W. Sollinger, Thermal analytical and infrared spectroscopic investigations on polymorphic organic compounds VIII, *Mikrochim. Acta* **102** (1990) 247, <https://doi.org/10.1007/BF01244766>
20. J. Pirsch, Polarity, molar heat of fusion, and melting-point position of organic compounds. Polymorphic transformations in the melting point region and their heats of transformation, *Monat. Chem.* **86** (1955) 216.
21. M. R. Caira, Crystalline polymorphism of organic compounds, *Topics in Current Chemistry* **198** (1998) 163, DOI: 10.1007/3-540-69178-2_5.
22. L. Yu *et al.*, hermochemistry and conformational polymorphism of a hexamorphic crystal system, *J. Am. Chem. Soc.* **122** (2000) 585, <https://doi.org/10.1021/ja9930622>
23. E. Ahmed, D. P. Karothu, L. Pejov, P. Commins, Q. Hu and P. Naumov, From mechanical effects to mechanochemistry: Softening and depression of the melting point of deformed plastic crystal, *J. Am. Chem. Soc.* **142** (2020) 11219, <https://dx.doi.org/10.1021/jacs.0c03990>
24. K. Salas-López, P. Amador, A. Rojas, F. J. Melende, and H. Flores, Experimental and theoretical thermochemistry of the isomers 3- and 4-nitrophthalimide, *J. Phys. Chem. A* **121** (2017) 5509, <https://doi.org/10.1021/acs.jpca.7b02508>
25. A. G. Abdul, A. Al-Muslem, N. Ahmad, A. Alquaity, U. Zahid and U. Ahmed, Predicting Enthalpy of Combustion Using Machine Learning, *Processes* **10** (2022) 2384, <https://doi.org/10.3390/pr10112384>
26. A. Vatani, M. Mehrpooya and F. Gharagheizi, Prediction of Standard Enthalpy of Formation by a QSPR Model, *Int. J. Mol. Sci.* **8** (2007) 407, <https://doi.org/10.3390/i8050407>
27. M. A. R. Matos, M. S. Miranda, D. A. P. Fonseca, V. M. F. Morais and J. F. Liebman, Calorimetric and Computational Thermochemical Study of 3,3-Tetramethyleneglutaric Acid, 3,3-Tetramethyleneglutaric Anhydride, and 3,3-Tetramethyleneglutarimide, *J. Phys. Chem A* **112** (2008) 10053, <https://doi.org/10.1021/jp805292x>
28. R. Sabbah *et al.*, Reference materials for calorimetry and differential thermal analysis, *Thermochim. Acta.* **331** (1999) 93, [https://doi.org/10.1016/S0040-6031\(99\)00009-X](https://doi.org/10.1016/S0040-6031(99)00009-X)
29. C. Plato and A. R. Glasgow, Differential scanning calorimetry as a general method for determining the purity and heat of fusion of high-purity organic chemicals. Application to 95 compounds, *J. Anal. Chem.* **41** (1969) 330, <https://doi.org/10.1021/ac60271a041>
30. M. E. Brown, Determination of purity by differential scanning calorimetry (DSC), *J. Chem. Educ.* **56** (1979) 310, <https://doi.org/10.1021/ed056p310>
31. P. Góralski, M. Tkaczyk and M. Chorazewski, Heat capacities of α,ω -dichloroalkanes at temperatures from 284.15 K to 353.15 K and a group additivity analysis, *J. Chem. Eng. Data.* **48** (2003) 492, <https://doi.org/10.1021/je020042y>
32. J. Coops, R. S. Jessup, K. G. van Nes and F. D. Rossini, Experimental Thermochemistry, *N. Y.: Interscience*, (1956).
33. D. D. Wagman *et al.*, The NBS tables of chemical thermodynamic properties: Selected values for inorganic and C₁ and C₂ organic substances in SI units, american chemical society and the american institute of physics for the national bureau of standards, Washington, D.C, (1982).
34. J. Meija *et al.*, Atomic weights of the elements 2013 (IUPAC Technical Report), *Pure Appl. Chem.* **88** (2016) 265, <https://doi.org/10.1515/pac-2015-0305>
35. W. D. Good, and N. K. Smith, Enthalpies of combustion of toluene, benzene, cyclohexane, cyclohexene, methylcyclopentane, 1-methylcyclopentene, and n-hexane, *J. Chem. Eng. Data* **14** (1969) 102, <https://doi.org/10.1021/je60040a036>
36. D. M. Price, Vapor pressure determination by thermogravimetry, *Thermochim. Acta* **367** (2001) 253, [https://doi.org/10.1016/S0040-6031\(00\)00676-6](https://doi.org/10.1016/S0040-6031(00)00676-6)
37. M.T. Vieyra-Eusebio and A. Rojas, Vapor Pressures and Sublimation Enthalpies of Nickelocene and Cobaltocene Measured by Thermogravimetry, *J. Chem. Eng. Data* **56** (2011) 5008, <https://doi.org/10.1021/je200815v>
38. M. A. García-Castro, P. Amador, J. M. Hernández-Pérez, A. E. Medina-Favela and H. Flores, Experimental and computational thermochemistry of 3- and 4-nitrophthalic anhydride, *J. Phys. Chem. A* **118** (2014) 3820, <https://doi.org/10.1021/jp5003929>
39. F. Ramos, J. M. Ledo, H. Flores, E. A. Camarillo, J. Carvente and M. P. Amador, Evaluation of sublimation enthalpy by thermogravimetry: Analysis of the diffusion effects in the case of methyl and phenyl substituted hydrantoin, *Thermochim. Acta* **655** (2017) 181, <https://doi.org/10.1016/j.tca.2017.06.024>
40. W. Acree and J. S. Chickos, Phase Transition Enthalpy Measurements of Organic and Organometallic Compounds. Sublimation, Vaporization and Fusion Enthalpies From 1880 to 2010, *J. Phys. Chem. Ref. Data* **45** (2016) 033101, <https://doi.org/10.1063/1.4948363>

41. A. Rojas and E. Orozco, Measurement of the enthalpies of vaporization and sublimation of solids aromatic hydrocarbons by differential scanning calorimetry, *Thermochim. Acta* **405** (2003) 93, [https://doi.org/10.1016/S0040-6031\(03\)00139-4](https://doi.org/10.1016/S0040-6031(03)00139-4)
42. R. Sabbah *et al.*, Reference materials for calorimetry and differential thermal analysis, *Thermochim. Acta* **331** (1999) 93, [https://doi.org/10.1016/S0040-6031\(99\)00009-X](https://doi.org/10.1016/S0040-6031(99)00009-X)
43. A. Rojas and M. T. Vieyra-Eusebio, Enthalpies of sublimation of ferrocene and nickelocene measured by calorimetry and the method of Langmuir, *J. Chem. Thermodyn* **43** (2011) 1738, <https://doi.org/10.1016/j.jct.2011.06.001>
44. R. S. Bradley and T. G. Cleasby, The vapour pressure and lattice energy of some aromatic ring compounds, *J. Chem.Soc.* **169** (1953) 1690, <https://doi.org/10.1039/JR9530001690>
45. C. G. De Kruijff, Enthalpies of sublimation and vapour pressures of 11 polycyclic hydrocarbons, *J. Chem. Thermodyn.* **12** (1980) 243, [https://doi.org/10.1016/0021-9614\(80\)90042-7](https://doi.org/10.1016/0021-9614(80)90042-7)
46. L. Malaspina, R. Gigli and G. Bardi, Microcalorimetric determination of the enthalpy of sublimation of benzoic acid and anthracene, *J. Chem. Phys.* **59** (1973) 387, <https://doi.org/10.1063/1.1679817>
47. P. C. Hansen and C. A. Eckert, An improved transpiration method for the measurement of very low vapor pressures, *J. Chem. Eng. Data* **31** (1986) 1, <https://doi.org/10.1021/je00043a001>
48. V. P. Klochov, The vapor pressure of some aromatic compounds, *Zh. Fiz. Khim* **32** (1985) 1177.
49. K. V. Zherikova and S. P. Verevkin, Ferrocene: Temperatura adjustments of sublimation and vaporization enthalpies, *Fluid Phase Equilib.* **472** (2018) 196, <https://doi.org/10.1016/j.fluid.2018.05.004>
50. A.S. Hukkerikar, R.J. Meier, G. Sin and R. Gani, A method to estimate the enthalpy of formation of organic compounds with chemical accuracy, *Fluid Phase Equilib.* **348** (2013) 23, <https://doi.org/10.1016/J.FLUID.2013.03.018>
51. N. Cohen, Revised group additivity values for enthalpies of formation (at 298 K) of carbon-hydrogen and carbon-hydrogen-oxygen compounds, *J. Phys. Chem. Ref. Data.* **25** (1996) 1411, <https://doi.org/10.1063/1.555988>
52. J. L. Holmes and C. Aubry, Group additivity values for estimating the enthalpy of formation of organic compounds: An update and reappraisal. 1. C, H and O, *J. Phys. Chem A* **115** (2011) 10576, <https://doi.org/10.1021/jp202721k>
53. E.S. Domalski and E.D. Hearing, Estimation of the Thermodynamic Properties of C-HN-O-S-Halogen Compounds at 298.15 K, *J. Phys. Chem. Ref. Data.* **22** (1993) 805, <https://doi.org/10.1063/1.555927>
54. R. Naef, A generally applicable computer algorithm based on the group additivity method for the calculation of seven molecular descriptors: heat of combustion, LogPo/w, LogS, refractivity, polarizability, toxicity and logbb of organic compounds; scope and limits of applicability, *Molecules* **20** (2015) 18279, <https://doi.org/10.3390/molecules201018279>
55. R. Naef and W.E. Acree Jr., Calculation of five thermodynamic molecular descriptors by means of a general computer algorithm based on the group-additivity method: standard enthalpies of vaporization, sublimation and solvation, and entropy of fusion of ordinary organic molecules and total phase-change entropy of liquid crystals, *Molecules* **22** (2017) 1059, <https://doi.org/10.3390/molecules22071059>
56. I. El Naqa and M.J. Murphy, What is machine learning?, *Machine Learning in Radiation Oncology: Theory and Applications* **17** (2015) 3, https://doi.org/10.1007/978-3-319-18305-3_1
57. X. Su, X. Yan and C.L. Tsai, Linear Regression, *WIREs Comput Stat* **4** (2012) 275, <https://doi.org/10.1002/wics.1198>
58. G.C. McDonald, Ridge Regression, *Inc. WIREs Comp Stat* **1** (2009) 93, <https://doi.org/10.1002/wics.14>
59. J. Ranstam and J.A. Cook, LASSO Regression, *British Journal of Surgery* **105** (2018) 1348, <https://doi.org/10.1002/bjs.10895>
60. J. D. Cox, D. D. Wagman and V. A. Medvedev, CODATA key values for thermodynamics *Hemisphere Pub. Corp.* (1989)
61. M. V. Roux, M. Temprado and J. S. Chickos, Vaporization, fusion and sublimation enthalpies of the dicarboxylic acids from C₄ to C₁₄ and C₁₆, *J. Chem. Thermodynamics* **37** (2005) 941, <https://doi.org/10.1016/j.jct.2004.12.011>
62. CAS Scifinder., Substance identifier (value calculated using Advanced Chemistry Development (ACD/Labs), Software V11.02 (©1994-2022 ACD/Labs) (2022)
63. C. Sousa, M. A. R. Matos and V. M. F. Morais, Experimental and Computational Thermochemical Study of Maleic Anhydride and Vinylene Carbonate, *J. Phys. Chem A* **121** (2017) 9474, <https://doi.org/10.1021/acs.jpca.7b07175>
64. Y. Meng-Yan and G. Plicher, Enthalpies of combustion of succinic anhydride, glutaric anhydride and glutarimide, *J.Chem. Thermodynamics* **22** (1990) 893, [https://doi.org/10.1016/0021-9614\(90\)90177-R](https://doi.org/10.1016/0021-9614(90)90177-R)
65. J. B. Pedley, R. D. Naylor and S. P. Kirby, Thermochemical Data of Organic Compounds, *computer analysed thermochemical data* **IV** (1986), <https://doi.org/10.1007/978-94-009-4099-4>
66. J. D. Cox and G. Plicher, Thermochemistry of organic and organometallic compounds, *NIST Chemistry Web Book* **69** (1970) 1.
67. W. V. Steele, R. D. Charico, A. B. Cowell, S. E. Knipmeyer and A. Nguyen, Thermodynamic Properties and Ideal-Gas Enthalpies of Formation for 1,4-Diisopropylbenzene, 1,2,4,5-Tetraisopropylbenzene, Cyclohexanone Oxime, Dimethyl Malonate, Glutaric Acid, and Pimelic Acid, *J. Chem. Eng. Data* **47** (2002) 725, <https://doi.org/10.1021/je010088b>
68. A. Vatani, M. Mehrpooya and F. Gharagheizi, Prediction of Standard Enthalpy of Formation by a QSPR Model, *Int. J. Mol. Sci* **8** (2007) 407, <https://doi.org/10.3390/i8050407>

69. B. Douglas, Computational Methods in Organic Thermochemistry. 2. Enthalpies and Free Energies of Formation for Functional Derivatives of Organic Hydrocarbons, *J. Org. Chem.* **72** (2007) 7313, <https://doi.org/10.1021/jo071213a>
70. M. A. V. Ribeiro da Silva, J. I. T. A. Cabral, P. Gomes and J. R. B. Gomes, Combined Experimental and Computational Study of the Thermochemistry of Methylpiperidines, *J. Org. Chem.* **71** (2006) 3677, <https://doi.org/10.1021/jo052468w>
71. W. Good, *J. Chem. Eng. Data* **17** (1972) 28.
72. S. P. Verevkin, *J. Chem. Thermodyn.* **29** (1997) 891.
73. P. Geladi and B.R. Kowalski, Partial least squares regression: a tutorial, *Anal Chim Acta* **187** (1986) 1.
74. A. Pendashteh *et al.*, Modeling of membrane bioreactor treating hypersaline oily wastewater by artificial neural network, *J. Hazard Mater* **192** (2011) 568, <https://doi.org/10.1016/j.jhazmat.2011.05.052>
75. T. Chai and R.R. Draxler, Root mean square error (RMSE) or mean absolute error (MAE)?, *Geosci. Model Dev. Discuss.* **7** (2014) 1525, <https://doi.org/10.5194/gmd-7-1247-2014>
76. Y. Jung, Multiple predicting K-fold cross-validation for model selection, *J. of Nonparametric Statistics* **30** (2018) 197, <https://doi.org/10.1080/10485252.2017.1404598>